

High-efficiency amorphous silicon solar cells: Impact of deposition rate on metastability

Takuya Matsui,^{1,a)} Adrien Bidiville,¹ Keigou Maejima,² Hitoshi Sai,¹ Takashi Koida,¹ Takashi Suezaki,^{2,3} Mitsuhiro Matsumoto,^{2,4} Kimihiko Saito,^{2,5} Isao Yoshida,² and Michio Kondo¹

¹National Institute of Advanced Industrial Science and Technology (AIST), 1-1-1 Umezono, Tsukuba, Ibaraki 305-8568, Japan

²Photovoltaic Power Generation Technology Research Association (PVTEC), 1-1-1 Umezono, Tsukuba, Ibaraki 305-8568, Japan

³Kaneka Corporation, 157-34 Kamiyoshidai, Toyooka, Hyogo 668-0831, Japan

⁴Panasonic Corporation, 3-4 Hikaridai, Seika-cho, Soraku-gun, Kyoto 619-0237, Japan

⁵Fukushima University, 1 Kanayagawa, Fukushima, Fukushima 960-1296, Japan

(Received 10 December 2014; accepted 19 January 2015; published online 2 February 2015)

Hydrogenated amorphous silicon (a-Si:H) films, used for light absorbers of p-i-n solar cells, were deposited at various deposition rates (R_d) ranging over two orders of magnitude ($R_d \sim 2 \times 10^{-3}$ – 3×10^{-1} nm/s) by using diode and triode plasma-enhanced chemical vapor deposition (PECVD). The impact of varying R_d on the light-soaking stability of the solar cells has been investigated. Although a reduction of R_d mitigates the light-induced degradation in the typical range of R_d ($>10^{-1}$ nm/s), it remains present even in the very low R_d ($<10^{-2}$ nm/s), indicating that the metastable effect persists in a-Si:H regardless of R_d . The best performing cell, whose a-Si:H absorber is characterized by low amount of metastable defect and high bandgap, can be obtained at R_d of ~ 1 – 3×10^{-2} nm/s by triode PECVD. By applying such a-Si:H in the improved p-i-n devices, we demonstrate two record independently confirmed stabilized efficiencies of 10.22% for single-junction and 12.69% for a-Si:H/hydrogenated microcrystalline silicon (μ c-Si:H) tandem solar cells.

© 2015 AIP Publishing LLC. [<http://dx.doi.org/10.1063/1.4907001>]

Hydrogenated amorphous silicon (a-Si:H) films are used as light absorbers for various types of thin-film silicon solar cells. In particular, a tandem device structure, which combines an a-Si:H top cell with a hydrogenated microcrystalline silicon (μ c-Si:H) bottom cell, is extensively applied in the industrial level. These solar cells suffer from the metastable light-induced degradation of a-Si:H known as the Staebler-Wronski effect.¹ Because of this adverse effect, the stabilized efficiency of the a-Si:H/ μ c-Si:H tandem solar cells after prolonged light illumination is limited to $\sim 12\%$,² although higher efficiency (14–15%) is achievable in the annealed (initial) state.^{3,4}

Deposition of the device-grade a-Si:H is generally carried out using a plasma-enhanced chemical vapor deposition (PECVD) technique with a standard parallel-plate electrode geometry (diode configuration). It is widely known that better light-soaking stability is attained in the relatively low-deposition-rate regime where a-Si:H is grown to exhibit less dihydride bonds (or hydrides at the surface of pores) and nano-sized voids, as revealed by infrared spectroscopy^{5,6} and positron annihilation spectroscopy.⁷ A recent electron-paramagnetic resonance study suggests that the metastable dangling bonds created at the internal surface of such voids play a role in light-induced degradation of a-Si:H.⁸ One of the origins of the porous microstructure observed in the high-deposition-rate regime is the incorporation of higher-order silane radicals and/or polyhydride nano-clusters

generated in high-density plasma. The contribution of these species with respect to the main precursor (i.e., SiH_3) has been reported as a factor that affects the metastability of a-Si:H.^{9,10} In order to reduce the incorporation of such unwelcome species during the a-Si:H deposition, a remote plasma process using a triode electrode configuration (see Fig. 1) has been proposed as a radical separation

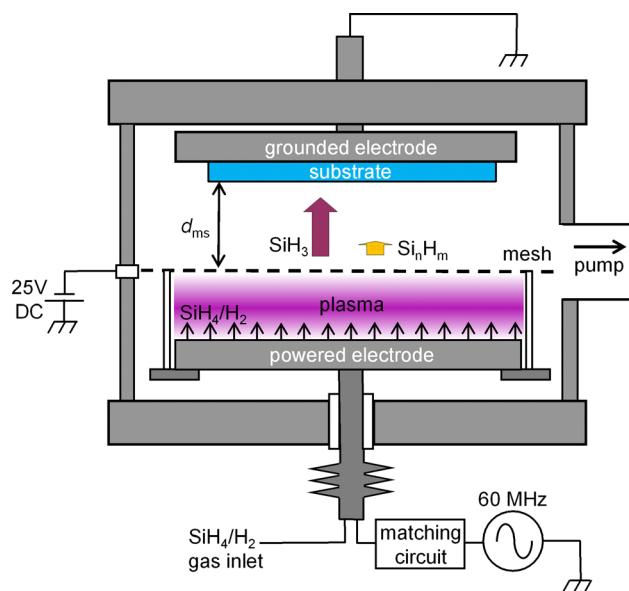


FIG. 1. A schematic illustration of the triode PECVD reactor used in this work. The a-Si:H deposition takes place mainly by the SiH_3 radical flux due to its longer diffusion than the higher-order silane radicals Si_nH_m ($n > 2$).

^{a)}Author to whom correspondence should be addressed. Electronic mail: t-matsui@aist.go.jp

technique,^{11–13} which provides a-Si:H films containing less dihydride bond density (<1 at. %). Although the deposition rate is relatively low in the triode PECVD ($<10^{-1}$ nm/s) compared to the conventional diode PECVD ($>10^{-1}$ nm/s), the light-induced degradation in conversion efficiency of single-junction a-Si:H solar cells has been substantially reduced.¹⁴ However, a question remains whether the improved metastability of a-Si:H prepared by the triode PECVD is attributed to the effect of the remote plasma process or to the lower deposition rate. In particular, the metastability of a-Si:H has not been studied in the lower deposition rates unavailable in the conventional diode PECVD.

In this work, we have investigated the impact of deposition rate of the a-Si:H absorber on the solar cell performance and its metastability. The deposition rate was varied over the wide range by using diode and triode PECVD processes. We show that the light-induced degradation does not disappear even when a-Si:H is deposited at very low deposition rates. Furthermore, we analyze the material properties such as defect, bandtail, and bandgap of a-Si:H deposited at various deposition rates. Finally, we demonstrate high-efficiency and stable solar cells based on single- and double-junction devices using the high-quality a-Si:H absorbers developed in this work.

Figure 1 shows a schematic illustration of the triode PECVD. A $\text{SiH}_4\text{-H}_2$ glow-discharge plasma was generated with a 60 MHz excitation at a power density (P_{rf}) of 30 mW/cm^2 , a gas pressure (P_g) of 0.15 or 0.05 Torr, and SiH_4/H_2 flow rates of 20/20 sccm. A mesh electrode was placed 20 mm above the powered electrode. A dc voltage of -25 V was applied to the mesh to confine the plasma between the powered and mesh electrodes. The substrates were mounted on a counter electrode which was electrically grounded and heated at $T_s = 210^\circ\text{C}$. The mesh electrodes with different aperture area ratios ($A_{\text{mesh}} = 5\%, 10\%, 30\%, \text{ and } 60\%$) were applied to vary the deposition rate (R_d) over a wide range. The distance between the mesh and substrate (d_{ms}) can be varied between 9 and 17 mm, enabling the additional adjustment of R_d without changing plasma-generation condition. The a-Si:H deposition with a diode electrode configuration was carried out by removing the mesh electrode. The distance between the powered and grounded electrodes (d) was fixed at 20 mm and the other parameters were unchanged except P_{rf} . In addition, a-Si:H films were deposited by another diode PECVD operated at a 13.56 MHz excitation frequency. The deposition parameters used in this process ($\text{SiH}_4/\text{H}_2 = 20/100$ sccm, $P_g = 1.0$ Torr, $T_s = 180^\circ\text{C}$, and $d = 15$ mm) were different from those used for 60 MHz because the optimum deposition condition depends markedly on the excitation frequency.

The undoped a-Si:H layers deposited by either triode or diode PECVD were incorporated as light absorbers (i layer) in p-i-n devices with a superstrate configuration (device area: 1.04 cm^2). For transparent conductive oxide (TCO) substrates, SnO_2 -coated glasses provided by Asahi Glass Company were used. The details of the TCOs, doped layers, and back contact designs can be found elsewhere.¹⁵ The current density-voltage (J - V) characteristics of the solar cells were measured under standard air mass 1.5 global

illumination (AM1.5G, 100 mW/cm^2 , cell temperature: $T_c = 25^\circ\text{C}$, and designated illumination area: 1.00 cm^2). As a stability test, the solar cells were exposed to AM1.5G illumination using a class A plasma-source solar simulator. The light-soaking experiment was carried out for 1000 h at $T_c = 50 \pm 1^\circ\text{C}$ in a controlled climate chamber. After the light-soaking stabilization, J - V characteristics of some samples were measured by the Calibration, Standards and Measurement Team, Research Center for Photovoltaic Technologies (CSMT-RCPVT) of AIST. Apart from the best performing devices, the most of the samples were exposed to 300 mW/cm^2 illumination at $T_c = 60^\circ\text{C}$ for 6 h used as a quick degradation test.¹⁴

Fourier transform photocurrent spectroscopy (FTPS)^{16,17} was applied to the p-i-n devices for measurement of the sub-bandgap absorption in the a-Si:H absorbers. The measurement setup used in this study has been reported in Ref. 18. The FTPS curves were calibrated using the corresponding external quantum efficiency (EQE) spectra measured in the photon energies of $E \geq 1.7 \text{ eV}$. Internal quantum efficiency (IQE) was then derived using the reflection spectrum of the corresponding cell in order to reduce the interference oscillations that appear in the low energy region.

Figure 2 shows the variation of R_d of a-Si:H prepared by (a) diode and (b) triode PECVD processes. For diode PECVD, R_d was varied from 5×10^{-2} to $3 \times 10^{-1} \text{ nm/s}$ by changing P_{rf} with two different excitation frequencies (13.56 and 60 MHz). As shown in Fig. 2(a), the lowest R_d of $\sim 5 \times 10^{-2} \text{ nm/s}$ is accessible for 13.56 MHz at low P_{rf} . With increasing P_{rf} , R_d increases and reaches the maximum of as high as $3 \times 10^{-1} \text{ nm/s}$ for both 13.56 and 60 MHz plasmas. In triode PECVD, as shown in Fig. 2(b), R_d was varied in the range from 2×10^{-3} to $5 \times 10^{-2} \text{ nm/s}$ by changing A_{mesh} from 5% to 60%. In addition, R_d was adjusted by varying d_{ms} . As a result, R_d was varied by two orders of magnitude using the diode and triode PECVD.

Figure 3 shows the solar cell parameters of the a-Si:H solar cells as a function of R_d in both diode and triode PECVD processes described above. The absorber thickness (t_i) was controlled to be between 210 and 260 nm in this

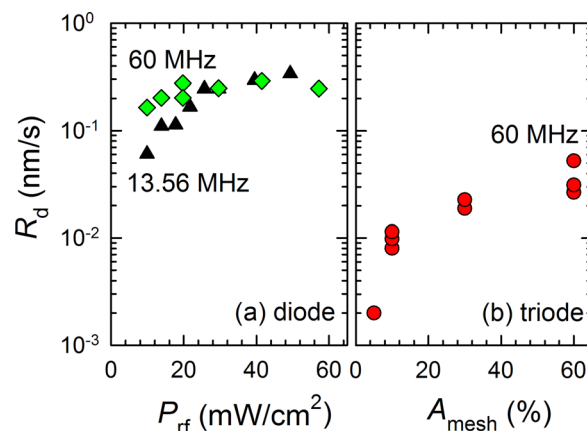


FIG. 2. Deposition rate (R_d) of a-Si:H prepared by (a) diode and (b) triode PECVD processes. In diode PECVD, R_d was varied by discharge power density (P_{rf}) with two different excitation frequencies (diamonds: 60 MHz and triangles: 13.56 MHz). In triode PECVD, R_d was varied by the aperture area ratio of the mesh electrode (A_{mesh}) and also by d_{ms} .

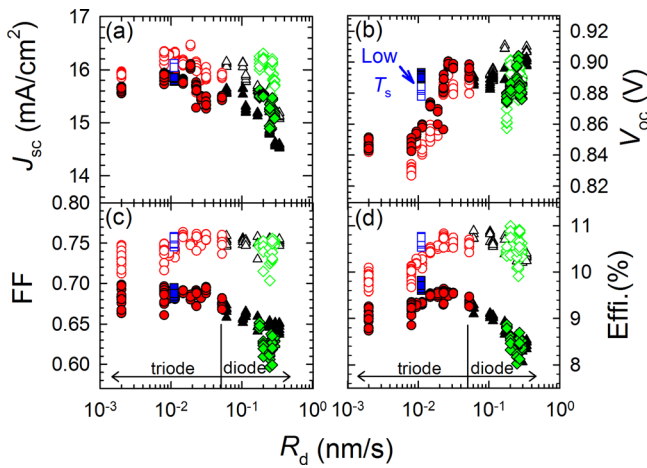


FIG. 3. Illuminated J - V parameters of the a-Si:H solar cells in the annealed (open symbols) and degraded (filled symbols, light soaking condition: AM1.5G, 300 mW/cm², $T_c = 60^\circ\text{C}$, 6 h, and open circuit) states as a function of R_d of the absorber layer deposited by triode (circles) and diode (diamonds: 60 MHz and triangles: 13.56 MHz) PECVD. (a) J_{sc} , (b) V_{oc} , (c) FF, and (d) efficiency. The J - V parameters of an improved cell, whose absorber layer was deposited at lower temperature ($T_s = 190^\circ\text{C}$) by triode PECVD, are shown by squares. The data include the results of seven cells fabricated in a substrate but exclude the shunted cell(s).

series. Exceptionally, the cell deposited at the lowest R_d of 2×10^{-3} nm/s has an absorber thickness of only 195 nm due to the poor thickness controllability because the deposition took a long time (27 h) with two intentional plasma stops. It should be noted that the plasma stops followed by long intervals of vacuum storage (approximately 15 h) does not deteriorate the solar cell performance, which was confirmed by applying the same process to the high efficiency solar cell prepared at higher R_d of 2×10^{-2} nm/s. In addition, we found that the reduction of R_d does not give rise to an enhanced impurity incorporation during deposition, as revealed by secondary-ion mass spectroscopy measurement for a-Si:H films deposited at various R_d (e.g., oxygen concentration is lower than 4×10^{19} cm⁻³ for R_d between 1.5×10^{-2} and 2.5×10^{-1} nm/s). In Fig. 3, solar cells prepared by the diode and triode PECVD cannot be compared except at $R_d \sim 5 \times 10^{-2}$ nm/s where the deposition rates of two techniques are nearly overlapped. Despite the different deposition techniques were used, clear trends are visible in solar cell parameters as a function of R_d . In both annealed and degraded states, the short-circuit current density (J_{sc}) tends to decrease at higher R_d in the diode regime ($R_d > 5 \times 10^{-2}$ nm/s), while the open-circuit voltage (V_{oc}) decreases at lower R_d in the triode regime ($R_d < 5 \times 10^{-2}$ nm/s). Fill factor (FF) and efficiency in the degraded state systematically decrease with increasing R_d in the diode regime, although the highest annealed efficiency of $\sim 11\%$ is attained at a typical R_d of $\sim 2 \times 10^{-1}$ nm/s. In triode regime, in contrast, the FF of ~ 0.7 after degradation is roughly independent of R_d . This indicates that there exists an upper limit of the degraded FF for single-junction solar cells with $t_1 \sim 200$ – 250 nm. The both annealed and degraded efficiencies become lower when $R_d < 2 \times 10^{-2}$ nm/s due to the low V_{oc} . This can be attributed to the reduced bandgap of the a-Si:H absorber layer. From the infrared absorption measurement, the hydrogen content in the a-Si:H is found to decrease

by ~ 1 at. % when decreasing R_d from 2.3×10^{-2} to 9.5×10^{-3} nm/s. This is because the hydrogen content is determined by competitive surface reactions, i.e., the rate of the precursor fluxes (such as SiH₃ and H) and the rate of the hydrogen desorption, if the deposition temperature is kept constant.¹² In fact, as shown in Fig. 3, the V_{oc} of a cell prepared at low rate ($R_d = 1.0 \times 10^{-2}$ nm/s) is markedly improved by lowering the T_s from 210 to 190 °C. Such cell shows the highest efficiency after light soaking.

Figure 4 shows the IQE spectra measured by FTPS for the a-Si:H solar cells in the annealed and degraded states. Here, we chose three distinct samples whose a-Si:H absorbers were deposited in the different deposition rate regimes (a very low R_d of 9.5×10^{-3} and a low R_d of 2.3×10^{-2} nm/s by triode, and a typical R_d of 2.7×10^{-1} nm/s by diode). In Fig. 4, the IQE spectrum is classified into three parts: absorption due to defect states for $E < 1.5$ eV, bandtail states for $E \sim 1.5$ – 1.7 eV, and extended states for $E > 1.7$ eV. In all cells, an increase of sub-bandgap absorption by a factor of 2–3 is observed for $E < 1.5$ eV after the light soaking, which is due to the creation of the light-induced metastable defects. Here, we define IQE at $E = 1.4$ eV as a measure of the amount of defects. From the bandtail states, the Urbach energy (E_u) was deduced using an exponential fit ($\text{IQE} \sim \exp(E/E_u)$). The bandgap (E_g) was determined by the spectroscopic ellipsometry using a Tauc-Lorentz model.¹⁹ These physical parameters of three samples are summarized in Table I, together with their solar cell parameters. In Table I, the defect absorption in the degraded state is lower by a factor of 1.5 for the cells

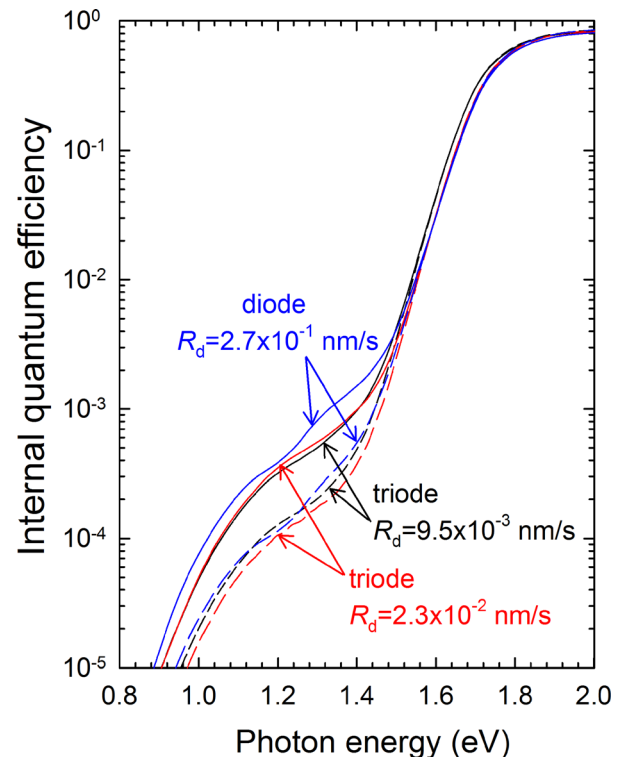


FIG. 4. IQE spectra obtained by FTPS ($E < 1.7$ eV), EQE ($E > 1.7$ eV), and optical reflection measurements for a-Si:H p-i-n solar cells whose absorber layers were deposited at different R_d by diode (60 MHz) and triode PECVD. The spectra of annealed (dashed lines) and degraded (solid lines, light soaking condition: AM1.5G, 300 mW/cm², $T_c = 60^\circ\text{C}$, 6 h, and open circuit) states are shown.

TABLE I. Parameters obtained from Fig. 4, IQE at $E = 1.4$ eV defined here as an amount of defect and Urbach energy (E_u), for a-Si:H solar cells prepared at various deposition rates (R_d) by diode (60 MHz) and triode PECVD in the annealed and degraded states (light-soaking condition: AM1.5G, 300 mW/cm², $T_c = 60^\circ\text{C}$, 6 h, and open circuit). J - V parameters of the corresponding solar cells are also shown. The bandgap (E_g) of a-Si:H layer deposited on glass substrate was estimated by spectroscopic ellipsometry using a Tauc-Lorentz model.

Reactor	R_d (nm/s)	t_i (nm)	States	IQE (1.4 eV)	E_u (meV)	E_g (eV)	J_{sc} (mA/cm ²)	V_{oc} (V)	FF	Effi. (%)
Diode	2.7×10^{-1}	235	Annealed	5.49×10^{-4}	43.0	1.69	16.1	0.896	0.756	10.9
			Degraded	1.51×10^{-3}	44.8	...	15.4	0.885	0.639	8.69
			Δ (%)	-4.35	-1.22	-15.5	-20.3
Triode	2.3×10^{-2}	236	Annealed	3.74×10^{-4}	39.6	1.69	16.1	0.885	0.761	10.8
			Degraded	9.85×10^{-4}	41.7	...	15.7	0.892	0.686	9.63
			Δ (%)	-2.49	+0.790	-9.86	-10.8
Triode	9.5×10^{-3}	241	Annealed	4.88×10^{-4}	39.2	1.67	16.3	0.848	0.745	10.3
			Degraded	9.72×10^{-4}	41.2	...	15.9	0.852	0.690	9.32
			Δ (%)	-2.45	+0.472	-7.38	-11.5

prepared by triode PECVD than that by diode PECVD. In particular, the lower defect absorption reflects the higher FF (~ 0.7) in the degraded states. This indicates that the light-induced degradation of a-Si:H solar cell is primarily governed by the amount of the metastable defects. In contrast, the variation of E_u is too small to account for the solar cell results in this series. We find that the bandgap has a rather big impact on the V_{oc} in both annealed and degraded states. The bandgap of the cell deposited at the lowest R_d is smaller by 20 meV than that of the others, in agreement with the redshift of the IQE spectrum as shown in Fig. 4. Consequently, this cell exhibits the lowest V_{oc} and the highest J_{sc} . However, the decrease of V_{oc} ($\Delta V_{oc} \sim 40$ mV) is greater than the decrease of the bandgap ($\Delta E_g \sim 10$ – 20 meV), resulting in the lower efficiency in spite of the low defect absorption. We attribute this to the presence of the bandtail states that hinder the quasi-Fermi level splitting as the E_g decreases. Another possible reason is the p-i interface damage during the low-rate deposition of a-Si:H on p-layer because a small decrease of the short wavelength response has been observed in EQE spectrum (not shown). On the other hand, the increase of V_{oc} by light soaking is found for the cells prepared by the triode PECVD. This effect has been explained by the Fermi-level shift near the p-i interface due to the metastable space charge generation in the i-layer.^{20,21}

As described above, the best performing a-Si:H solar cells are obtained in the middle range of deposition rate ($R_d \sim 1$ – 3×10^{-2} nm/s) by triode PECVD. By incorporating such high-quality material in our optimized device architecture¹⁵ with an antireflective film on glass,²² we have attained two high-efficiency solar cells measured by CSMT-RCPVT of AIST after light-soaking stabilization under the 1 sun illumination condition (AM1.5G, 100 mW/cm², 1000 h, $T_c = 50^\circ\text{C}$, and open-circuit). For single-junction device, an a-Si:H solar cell with $t_i \sim 220$ nm shows a stabilized efficiency of $10.22 \pm 0.3\%$ ($J_{sc} = 16.36$ mA/cm², $V_{oc} = 0.896$ V, and FF = 0.698). The relative efficiency degradation ($\Delta\eta/\eta$) of this solar cell was found to be 10%. This stabilized efficiency is higher than the previous record efficiency of 10.09% ($J_{sc} = 17.28$ mA/cm², $V_{oc} = 0.876$ V, and FF = 0.665) reported by Benagli *et al.*²³ Although these stabilized efficiencies are still comparable, our solar cell exhibits **higher stabilized FF, which can mainly be attributed to the improved metastability of the a-Si:H absorber layer**. For a-Si:H/ μ c-Si:H tandem solar

cells, we have made a progress from the previous report.¹⁴ In this work, the high-haze boron-doped ZnO²⁴ grown by our metalorganic chemical vapor deposition system²⁵ was used as front TCO instead of SnO₂ for better light trapping in the μ c-Si:H bottom cell. In our device, top-cell thickness was increased to 350 nm by taking advantage of the improved metastability of the a-Si:H absorber deposited by triode PECVD. In addition, a 50 nm-thick SiO_x intermediate reflector was applied to increase the top-cell current. The thicknesses of the bottom cell were 2.5 μ m. Such device shows a stabilized efficiency of $12.69 \pm 0.4\%$ ($J_{sc} = 13.45$ mA/cm², $V_{oc} = 1.342$ V, and FF = 0.702). This confirmed efficiency is slightly higher than the record cell reported recently by Boccard *et al.*²⁶ The solar cell exhibits degradation of only $\Delta\eta/\eta \sim 3\%$ according to our in-house J - V measurement.

In summary, we show that the amount of metastable defect in a-Si:H deposited by triode PECVD is smaller than that of diode PECVD, explaining the better solar cell performance after light soaking. As a result, we demonstrate high stabilized efficiencies in both single- and double-junction devices. Nevertheless, by varying the deposition rate of a-Si:H over the wide range using two deposition techniques, it appears that the triode PECVD process is not strikingly advantageous when compared to the cells deposited by diode PECVD at similar deposition rates. In contrast, it is found that the metastable effect persists and bandgap narrowing occurs in the very low deposition rate regime, leading to no further improvement in the solar cell performance. Further study is necessary to conclude the limits of the metastability in a-Si:H.

The authors are grateful to Mr. Miyagi, Murata, Sato, and Ms. Hozuki for the help in sample preparation, and to Dr. Hishikawa, Ms. Sasaki, and Mr. Shimura in CSMT-RCPVT of AIST for high accuracy J - V measurements. They are also grateful to the technical board member of PVTEC for discussion and continuous support. T.M. and A.B. especially thank researchers in EPFL and Delft University of Technology for technical discussion on FTPS measurement. This work was supported by the New Energy and Industrial Technology Development Organization (NEDO).

¹D. L. Staebler and C. R. Wronski, *Appl. Phys. Lett.* **31**, 292 (1977).

²For a review, see, e.g., A. Shah, E. Moulin, and C. Ballif, *Sol. Energy Mater. Sol. Cells* **119**, 311 (2013).

- ³K. Yamamoto, A. Nakajima, M. Yoshimi, T. Sawada, S. Fukuda, T. Suezaki, M. Ichikawa, Y. Koi, M. Goto, T. Meguro, T. Matsuda, M. Kondo, T. Sasaki, and Y. Tawada, *Sol. Energy* **77**, 939 (2004).
- ⁴M. Boccard, C. Battaglia, S. Hänni, K. Söderström, J. Escarré, S. Nicolay, F. Meillaud, M. Despeisse, and C. Ballif, *Nano Lett.* **12**, 1344 (2012).
- ⁵E. Bhattacharya and A. H. Mahan, *Appl. Phys. Lett.* **52**, 1587 (1988).
- ⁶T. Nishimoto, M. Takai, H. Miyahara, M. Kondo, and A. Matsuda, *J. Non-Cryst. Solids* **299–302**, 1116 (2002).
- ⁷J. Melskens, M. Schouten, A. Mannheim, A. S. Vullers, Y. Mohammadian, S. W. H. Eijt, H. Schut, T. Matsui, M. Zeman, and A. H. M. Smets, *IEEE J. Photovoltaics* **4**, 1331 (2014).
- ⁸M. Fehr, A. Schnegg, B. Rech, O. Astakhov, F. Finger, R. Bittl, C. Teutloff, and K. Lips, *Phys. Rev. Lett.* **112**, 066403 (2014).
- ⁹T. Takagi, R. Hayashi, G. Ganguly, M. Kondo, and A. Matsuda, *Thin Solid Films* **345**, 75 (1999).
- ¹⁰K. Koga, M. Kai, M. Shiratani, Y. Watanabe, and N. Shikata, *Jpn. J. Appl. Phys., Part 2* **41**, L168 (2003).
- ¹¹A. Matsuda, T. Kaga, H. Tanaka, and K. Tanaka, *J. Non-Cryst. Solids* **59–60**, 687 (1983).
- ¹²S. Shimizu, M. Kondo, and A. Matsuda, *J. Appl. Phys.* **97**, 033522 (2005).
- ¹³H. Sonobe, A. Sato, S. Shimizu, T. Matsui, M. Kondo, and A. Matsuda, *Thin Solid Films* **502**, 306 (2006).
- ¹⁴T. Matsui, H. Sai, K. Saito, and M. Kondo, *Prog. Photovoltaics: Res. Appl.* **21**, 1363 (2013).
- ¹⁵T. Matsui, A. Bidiville, H. Sai, T. Suezaki, M. Matsumoto, K. Saito, I. Yoshida, and M. Kondo, in *Symposium A – Film-Silicon Science and Technology*, edited by P. Stradins, R. Collins, F. Finger, N. Wyrsh, and A. Terakawa (*Mater. Res. Soc. Symp. Proc.*, 2014), Vol. 1666, p. a01.
- ¹⁶M. Vaneček and A. Poruba, *Appl. Phys. Lett.* **80**, 719 (2002).
- ¹⁷J. Holovský, A. Poruba, Z. Purkr, and M. Vaneček, *J. Non-Cryst. Solids* **354**, 2167 (2008).
- ¹⁸A. Bidiville, T. Matsui, and M. Kondo, *J. Appl. Phys.* **116**, 053701 (2014).
- ¹⁹G. Jellison and F. Modine, *Appl. Phys. Lett.* **69**, 371 (1996).
- ²⁰P. Siamchai and M. Konagai, in *Proceedings of 25th IEEE Photovoltaic Specialists Conference*, Washington, DC, 13–17 May 1996, pp. 1093–1096.
- ²¹M. Stuckelberger, Y. Riesen, M. Despeisse, J.-W. Schütt, F.-J. Haug, and C. Ballif, *J. Appl. Phys.* **116**, 094503 (2014).
- ²²H. Sai, T. Matsui, K. Matsubara, M. Kondo, and I. Yoshida, *IEEE J. Photovoltaics* **4**, 1349 (2014).
- ²³S. Benagli, D. Borrello, E. Vallat-Sauvain, J. Meier, U. Kroll, J. Hoetzel, J. Bailat, J. Steinhäuser, M. Marmelo, G. Monteduro, and L. Castens, in *Proceedings of the 24th European Photovoltaic Solar Energy Conference and Exhibition*, Hamburg, Germany, 21–25 September 2009, pp. 21–26.
- ²⁴S. Fäy, U. Kroll, C. Bucher, E. Vallat-Sauvain, and A. Shah, *Sol. Energy Mater. Sol. Cells* **86**, 385 (2005).
- ²⁵K. Maejima, T. Koida, H. Sai, T. Matsui, K. Saito, M. Kondo, and T. Takagawa, *Thin Solid Films* **559**, 83 (2014).
- ²⁶M. Boccard, M. Despeisse, J. Escarre, X. Niquille, G. Bugnon, S. Hänni, M. Bonnet-Eymard, F. Meillaud, and C. Ballif, *IEEE J. Photovoltaics* **4**, 1368 (2014).